IEEE Access
Multidisciplinary | Rapid Review | Open Access Journal

Received July 14, 2019, accepted July 29, 2019, date of publication August 2, 2019, date of current version August 16, 2019.

Digital Object Identifier 10.1109/ACCESS.2019.2932719

Data-Driven State of Health Estimation of Li-Ion Batteries With RPT-Reduced Experimental Data

JUNGSOO KIM[1], (Student Member, IEEE), HUIYONG CHUN[1], MINHO KIM[1], JUNGWOOK YU[1], KWANGRAE KIM[2], TAEGYUN KIM[2], AND SOOHEE HAN[1], (Senior Member, IEEE)

[1]Department of Creative IT Engineering, Pohang University of Science and Technology, Pohang 37673, South Korea
[2]Department of Electrical Engineering, Pohang University of Science and Technology, Pohang 37673, South Korea

Corresponding author: Soohee Han (soohee.han@postech.ac.kr)

This work was supported in part by the National Research Foundation of Korea (NRF) grant funded by the Korean Government (MSIT) under Grant 2019R1A2C2008637, in part by the Electronics and Telecommunications Research Institute (ETRI) grant funded by the Korean Government under Grant 19ZR1150, and in part by the Sports Promotion Fund of the Seoul Olympic Sports Promotion Foundation, Ministry of Culture, Sports and Tourism, under Grant 1375026841.

ABSTRACT In order to accurately estimate the state of health (SOH) of a Li-ion battery, a reference performance test (RPT) needs to be conducted between several charging/discharging cycles for obtaining accurate data concerning the battery capacity and degradation. However, it is not practical to perform RPTs frequently because they are time-consuming and expensive; moreover, the Li-ion battery undergoes unnecessary degradation during test operations. Therefore, the RPTs should be performed as infrequently as possible. In this paper, a neural network-based SOH estimation scheme with reduced experimental data measured by the RPT is proposed for achieving economic efficiency and mitigating the dispensable degradation being caused by additional experiments. For the RPT-reduced experimental data, the continuous SOH estimation problem is formulated into a classification problem. The neural network learns how to estimate the SOH values using short time-series voltage and current data, labeled as the corresponding SOH values by the RPTs. Even in the SOH regions, where the data are not labeled as any given class and there is no prior knowledge on the corresponding SOH, the proposed SOH estimation scheme works well by performing regression with the class probability distribution.

INDEX TERMS Li-ion battery, neural network, reference performance test (RPT), state of health (SOH).

I. INTRODUCTION

The advent of the eco-friendly era has placed electric vehicles (EVs) firmly in the spotlight. Consequently, rechargeable batteries, as the power sources of EVs, are attracting considerable attention. Li-ion batteries, in particular, have been extensively used in most EVs because of their high energy and power density [1]. However, as the careless use or abuse of them will probably affect their life span, and they are relatively expensive compared to other batteries, their secure and efficient management is very important. The state of health (SOH), which provides information on the life span of an Li-ion battery, is one of the most important indices for ensuring safety and efficiency of use. Hence, the accurate estimation of the SOH of an Li-ion battery, and the observation of its varying trend is critical for checking the occurrence of abnormal changes.

Although the SOH of a battery is not a strictly defined physical quantity, there are two commonly accepted definitions in the industry and academia: the ratio of its present total capacity to its initial one, and its present equivalent series resistance across every cell [2]. The test procedure for measuring such SOH information of a battery is reference performance test (RPT). The RPT is performed at regular intervals during life-cycle testing to characterize the degradation process [3]. It provides information which can represent the SOH of Li-ion batteries such as capacity, internal resistance, and AC impedance.

The studies on SOH estimation that have been conducted so far considered the RPT only as a test procedure to obtain reference value of capacity and internal resistance of a battery. Therefore, they performed RPTs frequently during the

The associate editor coordinating the review of this manuscript and approving it for publication was Xinyu Du.

This work is licensed under a Creative Commons Attribution 4.0 License. For more information, see http://creativecommons.org/licenses/by/4.0/

battery life-cycle test to acquire plenty of SOH information. However, in fact, there are various practical problems in performing frequent RPTs. First, performing frequent RPTs greatly increases the time and cost of battery life-cycle test. Generally, one RPT is designed in such a way that various subtests are conducted serially, and each subtest takes a long time. In particular, the subtest for measuring capacity of the battery takes few days because it performs constant current - constant voltage (CC-CV) charging and discharging at a very low C-rate. Since a battery life-cycle test involves several tens of RPTs, several weeks, even several months, are spent only to perform RPTs. This causes a major disadvantage for the battery field, where there is a continuing need to test newly developed batteries many times. Second, performing frequent RPTs causes unnecessary degradation on the Li-ion battery. The main purpose of the life-cycle test is to analyze the effect of various charging and discharging conditions such as C-rate, temperature and depth of discharge (DOD) on the battery degradation rate. Performing frequent RPTs can lead to unnecessary degradation on the batteries, which hinders the achievement of this purpose. Previous studies have considered the effect of RPTs on the battery degradation as ''negligible'', but in fact, it is considerable [4]. For these reasons, the RPT performing frequency must be reduced as much as possible to the extent that the desirable SOH information be used. This paper proposes a method for estimating SOH of an Li-ion battery based on the assumption that limited data is obtained through a small number of RPTs. This limited data is called ''RPT-reduced experimental data'' in this paper.

SOH can be estimated by various methods using the available measured data. For accurate SOH estimation, accurate physical models are required along with experimental data obtained through long and elaborate procedures. Hence, in order to construct an accurate estimation scheme, a very sophisticated mathematical model should be generated with well-selected parameters obtained from a well-organized experimental setup. Such conventional model-based approaches with equivalent circuit models (ECMs) and electrochemical models have been extensively used for estimating the SOH; however, the dynamics of an actual Li-ion battery system cannot be completely reflected by a rigorous mathematical model [5]–[9].

In order to overcome the model accuracy limitation imposed on model-based approaches, data-driven approaches have been developed. The data-driven approach such as the artificial neural network (ANN) can reflect certain unmodeled dynamics and system uncertainties that cannot be captured by model-based approaches. Various SOH estimation schemes based on the methods such as recurrent neural network (RNN), Gaussian process regression (GPR), support vector machine (SVM), and probabilistic finite state automata (PFSA) have been proposed [10]–[17]. However, they are not suitable for online application, or cover only rule-based operation profiles not dynamic driving ones. Even some of them have both limitations above at the same time. Most of all, they all require abundant reference data obtained by frequent RPTs. In other words, such SOH estimation schemes not only ignored the waste of time and cost due to frequent RPTs, but also used undesirable reference SOH information reflecting unnecessary degradation. Therefore, it is meaningful to develop an online SOH estimation scheme using RPT-reduced experimental data under dynamic operation.

In this paper, a neural network for SOH estimation using RPT-reduced experimental data is proposed for achieving economic efficiency and mitigating the dispensable degradation due to RPT operation. Because the paper focuses on demonstrating the possibility and effectiveness of estimating SOH with RPT-reduced experimental data and a simple algorithm, a basic neural network is employed as the estimation method. The neural network topology, in this work, is designed based on a multilayer perceptron (MLP). For RPT-reduced experimental data, a continuous SOH estimation problem is formulated into a classification problem with the given classes designated by the accurately measured SOH through RPT. From the short time-series voltage and current data labeled with the corresponding SOH values by RPTs, the patterns and relationships are learned by a neural network for association; i.e., the short time-series measured data and the corresponding SOH values are used as the inputs and desirable outputs of the neural network, respectively. In this paper, five SOH points are measured by RPT and designated as classes. Consequently, the proposed SOH estimation scheme learns how to classify the current SOH of an Li-ion battery using only the measurable data in commercial battery management systems (BMSs). Even in SOH regions, where the data is not labeled as any given class and there is no prior knowledge on the corresponding SOH, the proposed SOH estimation scheme works well by performing regression with the class probability distribution output by pre-trained network. In this study, simulated data reflecting the dynamic driving profile is used in addition to real experimental data for the rule-based operation profile. It is demonstrated that the SOH is estimated with about 1.6% of error for rule-based operation profiles, and about 0.5% of error for dynamic driving profiles. The key contributions of the proposed SOH estimation scheme can be summarized as follows:

- Accurate but slightly lacking reference SOH information obtained from a small number of RPTs is utilized.
- The cost and time for the entire battery life-cycle test including RPTs can be considerably saved through RPT-reduced experiment.
- Dynamic driving profiles are considered along with the rule-based operation ones.
- Suitable for online application because of low computational requirement of executing a pre-trained network.

The remainder of this paper is organized as follows: Section II presents the proposed estimation scheme and the relevant data. Section III establishes that the proposed scheme works well under both rule-based and dynamic driving operations. Finally, Section IV concludes the paper with a brief summary of the main contributions of the paper.

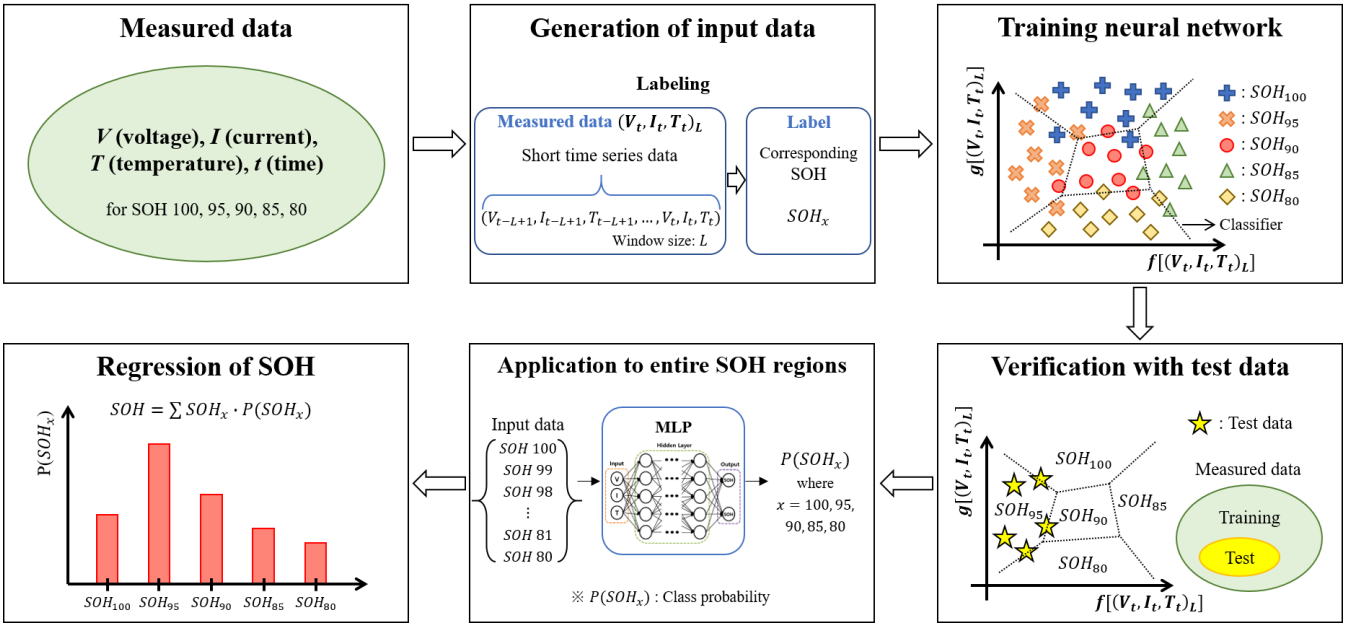

FIGURE 1. Procedure of the proposed SOH estimation scheme.

II. DATA-DRIVEN SOH ESTIMATION AND RELEVANT DATA

The overall procedure of the proposed SOH estimation scheme is shown in Fig.1. Initially, measured data such as the voltage, current, and temperature, in recent finite time, are grouped to form the input data for the neural network. They are then associated with labels denoted by their corresponding SOH values. The obtained input data enable the MLP learning process to perform iterative computation for extracting their features and clustering them accordingly, as shown in Fig.2. Further, the input data, which is not used for training, is applied to the MLP for validating the training. For SOH regions that do not belong to any given class, the class probability distribution is utilized for performing a regression of the corresponding SOH by computing its expected value. Details on the formation of the input data for the neural network, implementation of a neural network with multilayer perceptron, the conducted experiments and simulations for obtaining the necessary data, and SOH regression using the class probability distributions are presented below.

A. INPUT DATA FOR THE ARTIFICIAL NEURAL NETWORK

Data preprocessing is performed not only in the offline training stage but also in the prediction stage conducted by the BMS on a real-time basis. For avoiding heavy computation, only typical and simple methods, such as normalization and batch processing, are employed without advanced data preprocessing.

As the main idea behind the proposed scheme in this paper, we exploit time-series data, in recent finite time, for evaluating the extent of battery degradation. All the measured data in the SOH $x\pm0.05$ range are labeled as SOH_x. For example,

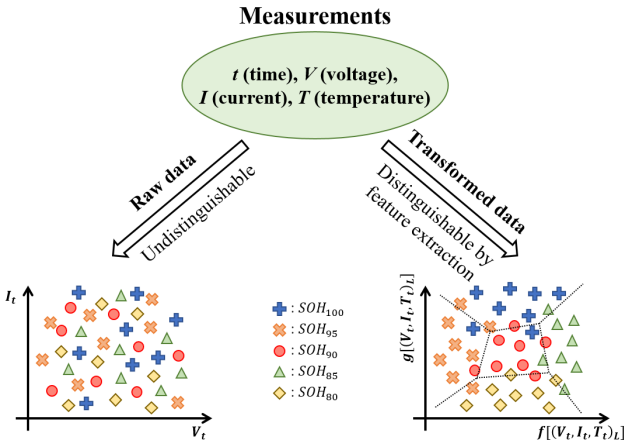

FIGURE 2. Neural network-based nonlinear transformation of the measured data.

the real SOHs of the input data labeled as SOH_{95} range from 94.95-95.05. Thereby, it is possible to extract multiple sets of short time-series data, which are sufficient for including the degradation dynamics of an Li-ion battery.

As shown in Fig.3, time-series data in recent finite time is taken according to the window size, and it moves sequentially by window stride. In the case of Fig.3, for example, data for L time-steps are determined as an input set, and this is repeated every m time-steps. The window size is selected to be L steps and there are three types of measured data: voltage, current, and temperature; hence, there are $3L$ elements in a single input set. Increasing the window size leads to abundant information, which is advantageous for the neural network for learning the degradation phenomena. It is because that the larger the size of the input data is, the more prominent

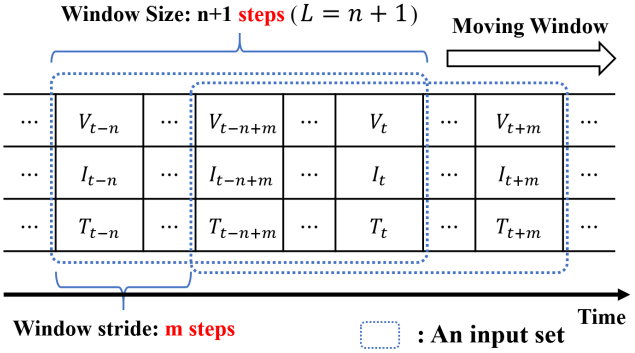

FIGURE 3. Short time-series measured data in recent finite time.

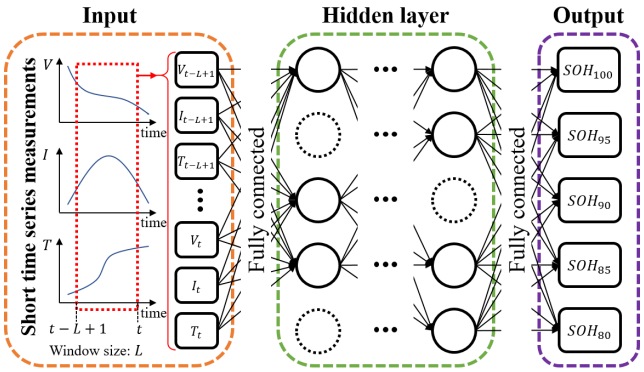

FIGURE 4. Overall view of the proposed multilayer perceptron. Dotted nodes indicate dropout.

is the feature that improves the classification performance of the neural network. However, as the window size increases, the time taken for preprocessing to make the raw data into form of neural network input becomes longer. Moreover, as the number of the nodes in the input layer increases, the number of the nodes in the hidden layer should be correspondingly increased, which requires larger memory and longer computation time for learning and testing. Above all, from the user's point of view, it is not practical to employ the large window size, because the minimum battery operation time to estimate the SOH becomes longer. Therefore, it is important to choose an appropriate value of the window size for sufficiently expressing the battery degradation dynamics, while achieving tolerable accuracy and computational complexity.

B. MULTILAYER PERCEPTRON

Data sets of the grouped measured data and their corresponding labels (SOHs) enable us to cast the SOH estimation problem of an Li-ion battery into a simple classification problem. A multilayer perceptron (MLP), which is a type of ANN, is adopted for solving this classification problem. The ANN represents a type of computing system inspired by the way brain performs computation [18]. The perceptron, which is the first form of ANN, consists of a single layer and has a binary activation function. As an advanced form of the perceptron, the MLP is multilayered and has a nonlinear activation function, which enable the MLP to reflect nonlinearities more effectively. The deeper the MLP layer, the more complex is the nonlinearity that it can express. Therefore, the MLP can even reflect certain unmodeled dynamics and system uncertainties that cannot be captured by model-based approaches.

Fig.4 shows the schematic of the MLP utilized in this paper. The MLP receives the short time-series measured data as the input and returns the corresponding SOH class. In order to suitably accommodate the nonlinearity of the battery dynamics, the MLP is designed as a form of deep neural network with two or more hidden layers. Hyperparameters, such as the number of hidden layers and the number of nodes in each hidden layer, should be determined appropriately. To render the training speed fast by reducing the internal covariate shift that often occurs in deep neural networks, the batch normalization technique is employed [19]. Dropout technique is also applied to reduce overfitting and improve regularization performance [20].

Instead of the sigmoid and hyperbolic tangent functions, a rectified linear unit (ReLU) function is generally used as the activation function in the hidden layers of a deep neural network for alleviating vanishing gradient problems [21]. The proposed scheme also adopts the ReLU as the activation function in the hidden layers. In order to compute the class probability, the softmax function is employed in the output layer, and it returns the probabilities of the input data belonging to each of the classes.

Although certain time is required for training the network, once the training is complete, the pre-trained network becomes a feedforward network with low computational requirement, performing only simple algebraic calculations.

C. RULE-BASED OPERATION PROFILES

For effective training of the MLP over long life-cycles, the life-cycle data requirement is demanding. For convenience, the charging/discharging operation is often scheduled by predetermined conditions, which do not appropriately reflect dynamic driving. The creation of dynamic driving profiles is discussed later. The battery and experimental settings used for the rule-based life-cycle test are as follows:

The 18650-type cylindrical lithium nickel manganese cobalt oxide (NMC) cells were employed for the life-cycle test. The initial capacity of the cells was 2000 mAh at 25ÂřC and the nominal voltage was 3.6 V. The test cycle consists of the charging/discharging and RPT sections. The charging/discharging profiles were designed using certain predetermined rules as shown in Table 1. In charging operation, the battery cell was charged in the CC mode until its terminal voltage reached the cut-off voltage; it was then switched to the CV mode and charged until its current reached the cut-off current. In discharging operation, the cell was discharged in the CC mode until its terminal voltage reached the cut-off voltage. The 10 minutes of resting follows right after

TABLE 1. Design of experiment (DOE) for rule-based profiles.

	Settings	Cell#1, Cell#2	Cell#3
Charging	C-rate	1C	1C
	Cut-off voltage	4.1V	4.1V
	Cut-off current	145mA	145mA
	Rest time	10min	10min
Discharging	C-rate	0.5C	1C
	Cut-off voltage	3.0V	3.0V
	Rest time	10min	10min

TABLE 2. Configuration and duration of RPT.

Test	Sequence	Duration
Initialization	1C charge	1H
	Rest	1H
Capacity measurement	C/25 discharge	25H
	Rest	1H
	C/25 charge	25H
	Rest	1H
Total		54H

every charging/discharging operations. In case of cell#1, for example, the C-rate and cut-off voltage for CC charging mode were set to 1 C and 4.1 V, respectively, and the cut-off current for CV charging mode was 145 mA. The C-rate and the cut-off voltage for CC discharging mode were selected to be 1 C and 3.0 V, respectively. During the life-cycle test, the ambient temperature in the thermohygrostat chamber was controlled to be constant at 25ÂřC. In the experiment, the temperature of the cell was not measured, and hence only the voltage and current measurements were obtained.

Every several charging/discharging cycles, the RPT was performed for measuring the capacity of the battery cell. Typically, an RPT consists of various test sequences such as initialization, capacity measurement, electrochemical impedance spectroscopy (EIS), and low-current hybrid pulse power characterization (L-HPPC). In this study, only the initialization and the capacity measurement tests were conducted as RPTs. Table 2 shows the detail on the configuration and duration of an RPT.

The proposed scheme only requires measured data corresponding to certain SOH regions, not over the entire life span. In this paper, data for SOHs of 100, 95, 90, 85, and 80 are used. As mentioned earlier, the SOH indices are determined based on the currently available capacity of the Li-ion cell. Here, SOH 100 represents a fresh battery cell, which has an available capacity of 2000 mAh, and SOH 80 indicates that the available capacity is 80% of the initial available capacity, representing a fully-aged battery cell.

The Li-ion battery life-cycle data were provided by Samsung SDI Company Ltd. In addition to training the MLP with rule-based operation profiles, the provided data can be used to construct a model for generating dynamic driving profiles, as discussed subsequently in further detail.

D. DYNAMIC DRIVING PROFILES

From the available experimental data based on rule-based operation profiles, a mathematical model was constructed, and a new data set was generated through simulation for reflecting the dynamic driving profiles. Such a data generation method for dynamic driving profiles is outlined in Fig.5. The details of the parameterized models for each SOH region and a real input current profile are given below.

1) PARAMETERIZED MODELS

Pseudo 2-dimensional (P2D) model, a rigorous battery model developed based on physical principles, was adopted to generate the data for the dynamic driving profiles [7], [22]–[25]. LIONSIMBA, an Li-ion battery simulation toolbox based on MATLAB, was employed to simulate the dynamic driving operation [26]. To identify parameters for each SOH region, harmony search (HS) method, a well-known meta-heuristic algorithm, was utilized with the corresponding rule-based operation profiles, as shown in Fig.5(a). The model parameters for each of the five SOH regions, SOH 100, 95, 90, 85, and 80, were identified.

2) INPUT CURRENT PROFILE

Fig.5(b) shows the generating process for the dynamic driving profiles. In order to consider the dynamic driving patterns,

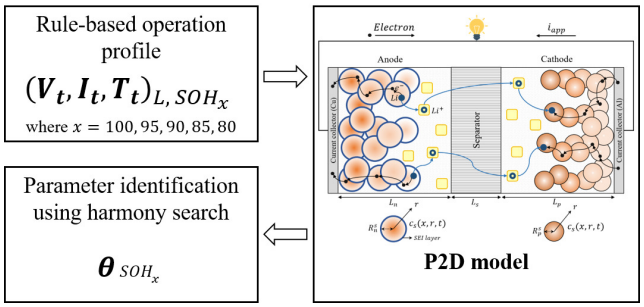

(a) Estimation of the P2D model parameters

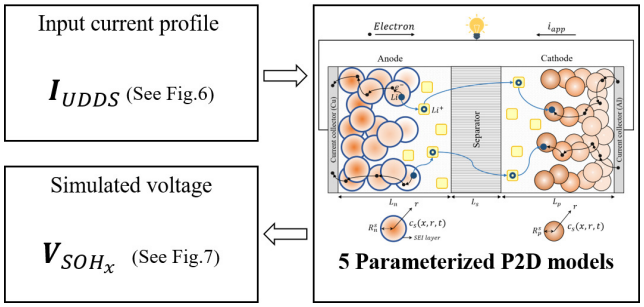

(b) Dynamic driving profiles generated from UDDS-cycled data

FIGURE 5. Dynamic driving profiles obtained from rule-based operation profiles through P2D model.

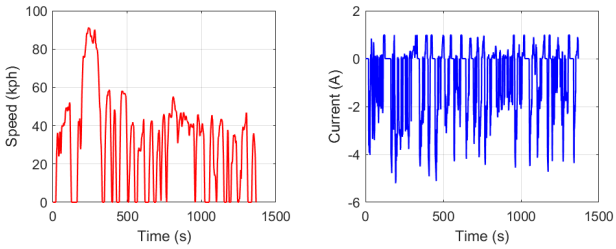

(a) Speed profile (b) Current profile

FIGURE 6. Transformation of the UDDS speed profile into a current profile.

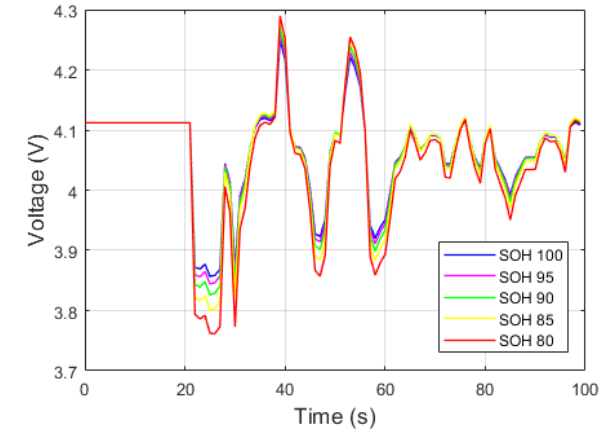

(a) Simulated output voltage

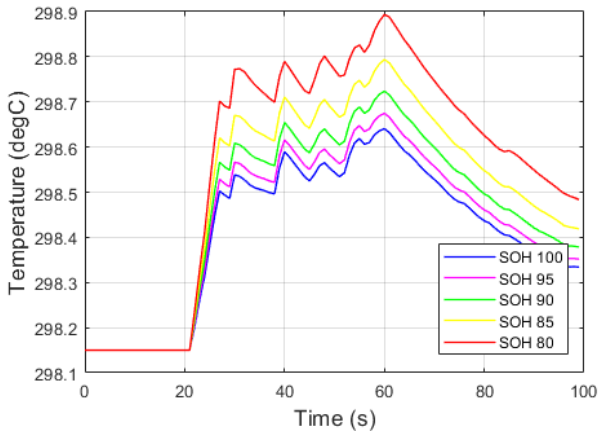

(b) Simulated output temperature

FIGURE 7. Li-ion cell simulation output voltage and temperature profiles under UDDS driving pattern. The first 100s of data for a total of 7000s is plotted.

the urban dynamometer driving schedule (UDDS) generated by the United States environmental protection agency (EPA) was employed [27]. The UDDS profile is composed of vehicle speeds, under city driving conditions. The input current profile was generated by transforming the speed values of the UDDS into current values. Fig.6 shows the UDDS profile and its transformation into a current profile.

The current profile shown in Fig.6(b) was applied to the parameterized P2D models. The output voltage and temperature profiles for the five SOH regions are shown in Fig.7(a) and Fig.7(b), respectively.

E. SOH REGRESSION

$$P_{mean,k} = \frac{1}{N}\sum_{n=1}^{N}\left(\frac{e^{\mathbf{x_n}^T \mathbf{w}_k}}{\sum_{j=1}^{5} e^{\mathbf{x_n}^T \mathbf{w}_j}}\right). \quad (1)$$

$$\mathbf{E}_{SOH} = \mathbf{SOH}^T \cdot \mathbf{P}_{mean}. \quad (2)$$

$P_{mean,k}$: *mean value of probability belonging to class k for all input sets*

N : *number of input sets*

$\mathbf{x}$: *input vector of output layer*

$\mathbf{w}$: *weight matrix between last hidden layer and output layer*

$\mathbf{E}_{SOH}$: *expectation of SOH*

$\mathbf{SOH}$: *vector of SOH values for given classes*

$\mathbf{P}_{mean}$: *vector of* $P_{mean,k}$ *for* $k = 1, \ldots, 5$

The MLP classification algorithm outputs the probability distribution over the classes to which the input data belong, based on the softmax function. If the SOH of an Li-ion battery does not belong to any of the classes designated in the training phase, the results from this classification algorithm can be used for regression. The final SOH value is obtained by considering an expectation with the class probability distribution, as shown in (1) and (2).

III. VALIDATION

For validating the proposed SOH estimation scheme, the data generation, preprocessing, and result analysis are implemented using MATLAB, whereas the MLP design and its training are implemented using Tensorflow.

A. MLP TRAINING

The parameters for the proposed MLP are listed in Table 3. As previously mentioned, there are three types of measured data: voltage, current, and temperature. The window size L is set to 180 steps; hence, the number of nodes in the input layer should be 540, according to Fig.3. In case of rule-based operation profile, as mentioned in Sections II-*C*, the temperature of the battery cell was not measured.

TABLE 3. Proposed MLP configuration.

Parameter	Rule-based	Dynamic driving
Window size (L)	180 steps	180 steps
Window stride	10 steps	3 steps
# of training sets	25305	9665
# of testing sets	4465	1705
Batch size	2048	256
Dropout rate	0.3	0.3
Learning rate	1.00E-04 to 1.00E-06	1.00E-06
# of nodes in I/O layer	360 / 5	540 / 5
# of hidden layers	4	3
# of nodes in each layer	2048, 1024, 512, 256	2048, 1024, 512

Therefore, only the voltage and current data are utilized as the input of the MLP algorithm; hence, an input set of rule-based operation profile has 360 nodes. 85% of the total input sets preprocessed as described in Section II-*A* are used for training, and the remaining 15% are used for testing. In addition, the other input sets that do not belong to the five SOH regions used for training are utilized for evaluating the SOH regression.

The classification results for the five SOH regions that belong to given classes are described, and the regression solutions for the sixteen SOH regions that do not belong to any class are presented subsequently along with their probability distributions. All the validations are carried out for both rule-based operation and dynamic driving profiles.

B. TEST RESULTS FOR THE FIVE SOH REGIONS BELONGING TO THE GIVEN CLASSES

For the input sets of the five SOH regions belonging to the given classes, the probabilities of belonging to each class, i.e., the softmax outputs, are shown in Fig.8. For the rule-based operation profiles, the class probabilities of all the input sets are averaged in each bar chart, as seen in Fig.8(a). In case of SOH 100, the probability of belonging to SOH_{100} is considerably higher than those belonging to the other classes, as seen in the first plot in Fig.8(a). This indicates that most of the input sets are classified correctly. For the dynamic driving profiles, the mean values of the class probabilities of all the input sets are plotted as shown in Fig.8(b). Compared to Fig.8(a), the dynamic driving profiles can be classified with higher accuracy.

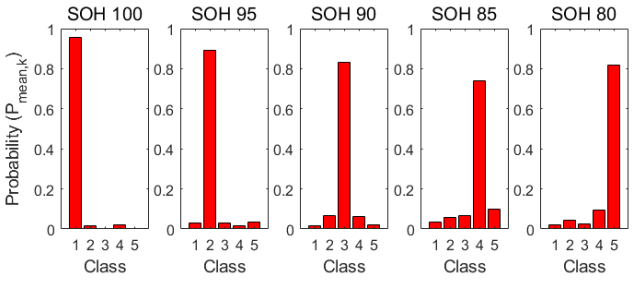

(a) Class probability distributions with rule-based operation profiles

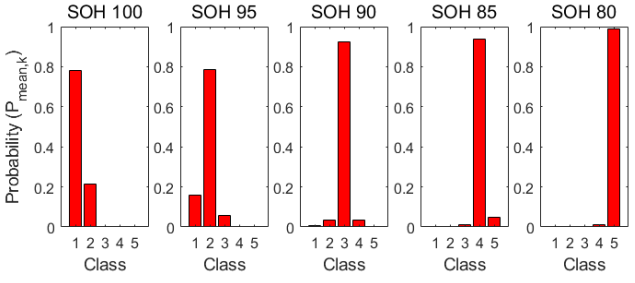

(b) Class probability distributions with dynamic driving profiles

FIGURE 8. Class probability distributions of the five SOH regions belonging to the given classes (Class information: Class 1: SOH_{100}, Class 2: SOH_{95}, Class 3: SOH_{90}, Class 4: SOH_{85}, and Class 5: SOH_{80}).

C. TEST RESULTS FOR THE SIXTEEN SOH REGIONS THAT DO NOT BELONG TO THE GIVEN CLASSES

As mentioned earlier, it is confirmed that the proposed MLP classifies the data of the trained SOH regions satisfactorily. Further, the proposed MLP is evaluated for the sixteen SOH regions that do not belong to any given class, namely, SOH 100, 95, 90, 85, and 80. Therefore, additional data was selected from the rule-based operation profiles to confirm that the proposed MLP trained with five SOH regions can be utilized in other SOH regions. Data corresponding to SOH 99–96, 94–91, 89–86, and 84–81 were selected. For the dynamic driving profiles, new input sets based on mathematical models were generated for these sixteen SOH regions according to the method described in Sections II-*A* and II-*D*.

Fig.9 shows the probabilities that the input sets of the sixteen SOH regions, which do not belong to the given classes, belong to each class. For the rule-based operation profiles, the class probabilities of all the input sets are averaged in each bar chart, as seen in Fig.9(a). In the case of SOH 97, the probabilities of belonging to SOH_{100} and SOH_{95} are higher than those of belonging to the other classes, as seen in the third plot of Fig.9(a). Theoretically, the class probability

TABLE 4. Estimated SOH for the rule-based operation profiles.

Input data	True SOH	Est. SOH	Error(%)
Belonging to the given classes	100	99.41	0.58
	95	94.50	0.52
	90	89.83	0.19
	85	85.79	0.93
	80	81.92	2.40
Not belonging to the given classes	99	97.88	1.13
	98	95.57	2.48
	97	94.01	3.08
	96	93.98	2.10
	94	93.43	0.60
	93	91.40	1.72
	92	90.40	1.74
	91	89.58	1.56
	89	89.74	0.83
	88	88.76	0.86
	87	88.40	1.60
	86	86.96	1.12
	84	85.29	1.53
	83	85.00	2.41
	82	85.11	3.80
	81	82.85	2.29
Mean error (%)		1.60	
Maximum error (%)		3.80	

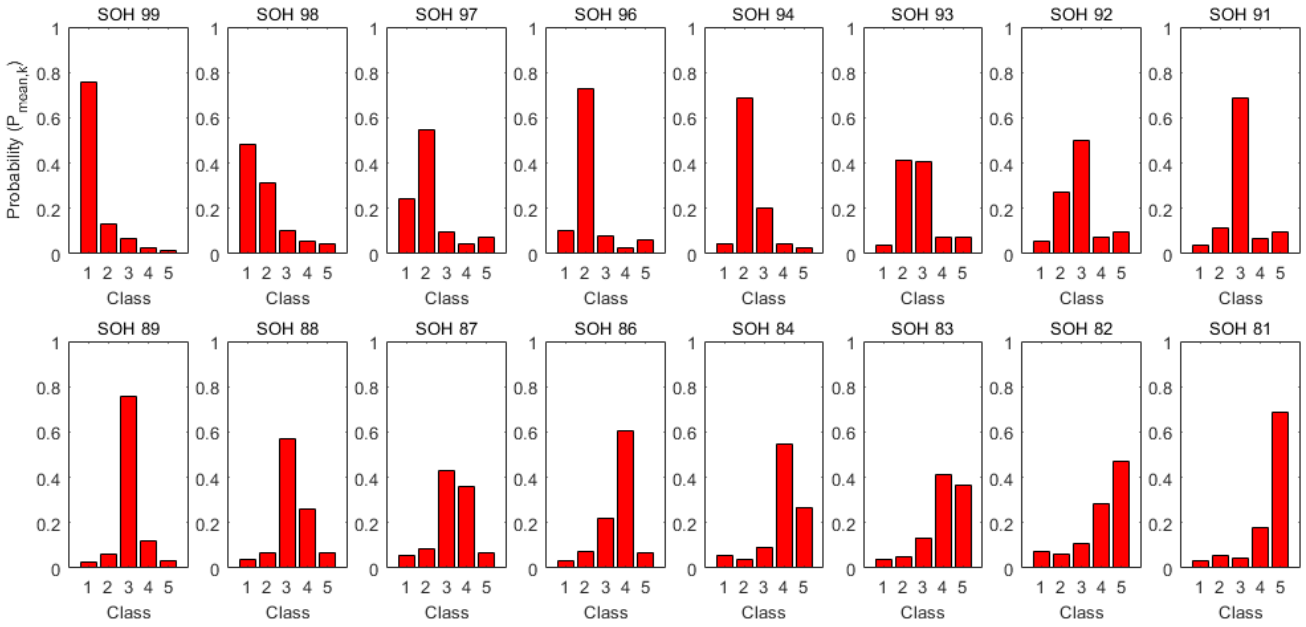

(a) Class probability distributions with rule-based operation profiles

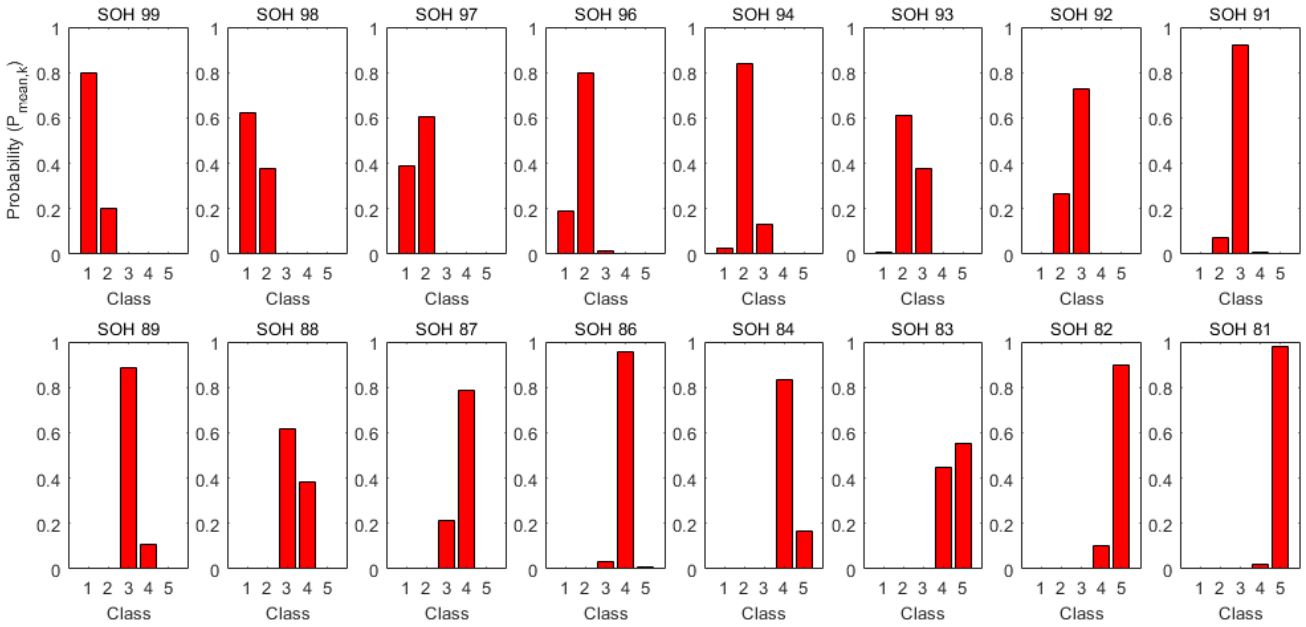

(b) Class probability distributions with dynamic driving profiles

FIGURE 9. Class probability distributions of the sixteen SOH regions that do not belong to the given classes (Class information: Class 1: SOH_{100}, Class 2: SOH_{95}, Class 3: SOH_{90}, Class 4: SOH_{85}, and Class 5: SOH_{80}).

distribution for the data of SOH 97 should be weighted to class 1 and 2; that is SOH 100 and SOH 95. Therefore, it can be considered that the results in Fig.9(a) are reasonable. The other cases show similar trends. For the dynamic driving profiles, the mean values of the class probabilities of all the input sets are plotted, as shown in Fig.9(b). The softmax outputs for the dynamic driving profiles show similar trends as Fig.9(a).

D. SOH REGRESSION

Based on the test results in Section III-*B,C* and the regression described in Section II-*E*, the SOH values corresponding to each input data are estimated and averaged as shown in Table 4 and Table 5.

The mean estimation errors for the SOH regions belonging to the given classes are about 0.93% for the rule-based operation profiles, and about 0.19% for the dynamic driving

TABLE 5. Estimated SOH for the dynamic driving profiles.

Input data	True SOH	Est. SOH	Error(%)
Belonging to the given classes	100	99.48	0.52
	95	95.17	0.18
	90	89.95	0.05
	85	84.82	0.21
	80	80.01	0.02
Not belonging to the given classes	99	98.98	0.02
	98	98.08	0.09
	97	96.91	0.09
	96	95.87	0.13
	94	94.46	0.49
	93	93.14	0.15
	92	91.33	0.73
	91	90.32	0.75
	89	89.48	0.54
	88	88.09	0.11
	87	86.04	1.11
	86	85.11	1.03
	84	84.17	0.20
	83	82.20	0.96
	82	80.47	1.87
	81	80.08	1.14
Mean error (%)		**0.49**	
Maximum error (%)		**1.87**	

profiles. The estimation errors for SOH regions that do not belong to the given classes are about 1.80% for the rule-based operation profiles, and about 0.59% for the dynamic driving profiles. The overall SOH estimation errors for rule-based operation profiles and dynamic driving profiles are about 1.60% and 0.49%, respectively. In summary, it is demonstrated that the SOH can be estimated with high accuracy for any SOH region using the MLP trained with RPT-reduced experimental data.

The estimation results for the dynamic driving profiles are better than those for the rule-based operation profiles. This can be explained with two major reasons. First, the rule-based profile has very little excitation because of its static input current. In particular, the current profile in constant current (CC) mode and the voltage profile in constant voltage (CV) mode, which account for most of the entire profile, are dummy measurements that does not contain sufficient information. In this case, the neural network is less likely to capture the data features. This can be interpreted by a perspective similar to the persistent excitation (PE) condition often encountered in control engineering. Second, while the dynamic driving profile consists of current, voltage, and temperature measurements, the rule-based profile only consists of two measurements, current and voltage, as noted in Section II-*C*.

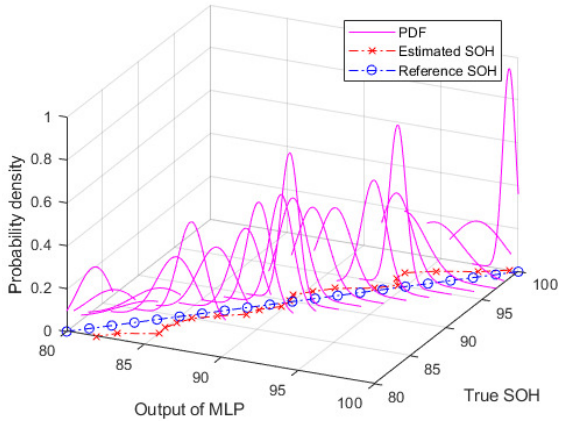

(a) Probability distribution with rule-based operation profiles for all SOH regions

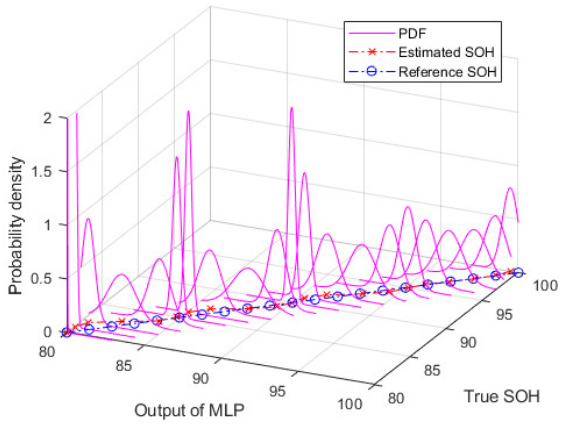

(b) Probability distribution with dynamic driving profiles for all SOH regions

FIGURE 10. Estimation results and reliability for all SOH regions in each profile.

Therefore, it can be interpreted that the neural network extracts the feature well from the dynamic driving profile which has more information, resulting in better estimation results.

In order to visualize the accuracy and reliability of the proposed SOH estimation scheme, the experimental results and probability distributions are shown in Figs.10. In both figures, the crossed and circled points, which represent the estimated SOHs and the true ones (references), respectively, depict the accuracy of the proposed algorithm. The solid line indicates the reliability of the algorithm and represents the distribution of the SOH expectations for all the input sets in each group. The distributions are fitted with a Gaussian distribution. From Fig.10(a), it can be observed that the variances of estimated SOH for rule-based operation profiles are small at all SOH regions. From Fig.10(b), it is also shown that the variances of estimated SOH for dynamic driving profiles are even smaller than those for rule-based operation profiles at all SOH regions. Based on these results, it can be concluded that the proposed SOH estimation algorithm is highly reliable over the entire life span.

TABLE 6. Economic comparison between life-cycle tests with frequent RPTs and RPT-reduced life-cycle tests.

	Life-cycle tests with frequent RPTs			RPT-reduce life-cycle tests			
Cell	Cycle duration [days]	RPT duration [days]	Total [days]	Cycle duration [days]	RPT duration [days]	Total [days]	Time saved [days]
Cell#1	203.80	47.25 (21 RPTs)	251.05	203.80	11.25 (5 RPTs)	215.05	**36.00 (14.3%)**
Cell#2	216.36	49.50 (22 RPTs)	265.86	216.36	11.25 (5 RPTs)	227.61	**38.50 (14.4%)**
Cell#3	103.29	27.00 (12 RPTs)	130.29	103.29	11.25 (5 RPTs)	114.54	**15.75 (12.1%)**

E. EFFECT OF RPT-REDUECD LIFE-CYCLE TESTS

In the previous section, it is confirmed that the SOHs of Li-ion batteries can be accurately estimated with RPT-reduced experimental data. It is then necessary to analyze how much the RPT-reduced life-cycle test has an effect in economic perspective. Table 6 shows the detail on economic evaluation for RPT-reduce life-cycle tests.

The part 'Life-cycle tests with frequent RPTs' in Table 6 represents the time spent in actual rule-based operation life-cycle tests. The part 'RPT-reduced life-cycle test' in Table 6 represents the time spent assuming the RPT-reduced life-cycle tests were performed. As shown in Table 6, it is possible to achieve more than 10% of time saving effect by adopting RPT-reduced life-cycle tests.

IV. CONCLUSION

A practical SOH estimation scheme with RPT-reduced experimental data was proposed in this paper. This study proves that it is possible to estimate the SOH using Li-ion battery life-cycle data, with only a few RPTs. Therefore, the proposed data-driven SOH estimation scheme can mitigate the dispensable degradation caused by RPT and also can save the cost and time for the entire battery life-cycle test. Additionally, the dynamic driving profile is considered using a driving profile, which is advantageous for practical application. The proposed algorithm exhibits highly accurate SOH estimation results: about 98.4% for rule-based operation profiles, and about 99.5% for dynamic driving profiles. It was also observed that the proposed algorithm can be utilized even for data that the MLP does not experience.

This paper establishes that SOH estimation with RPT-reduced experimental data is achievable using only a basic neural network; even a simple neural network can extract the features of the degradation mechanism of an Li-ion battery. In future, advanced neural network or other data-driven techniques need to be developed, which can reflect the Li-ion battery's degradation dynamics more efficiently and accurately. It should be considered whether such techniques meet the computational requirements for cost-effective hardware resources of a BMS. Furthermore, if it is possible to reduce the overall experiment time through the proposed method with RPT-reduced experimental data and instead spend more time in accumulating large amounts of data through various battery-related infrastructures to be built in the near future, more rigorous and robust algorithms covering various operating conditions can be developed.

REFERENCES

[1] H. Rahimi-Eichi, U. Ojha, F. Baronti, and M.-Y. Chow, "Battery management system: An overview of its application in the smart grid and electric vehicles," *IEEE Ind. Electron. Mag.*, vol. 7, no. 2, pp. 4–16, Jun. 2013.
[2] G. L. Plett, *Battery Management Systems: Equivalent-Circuit Methods*, vol. 2. Norwood, MA, USA: Artech House, 2015.
[3] G. Hunt and C. Motloch, "Freedom CAR battery test manual for power-assist hybrid electric vehicles," INEEL, Idaho Falls, ID, USA, Tech. Rep. DOE/ID-11069, 2003, ch. 4.11.
[4] J. P. Christophersen, C. D. Ho, C. G. Motloch, D. Howell, and H. L. Hess, "Effects of reference performance testing during aging using commercial lithium-ion cells," *J. Electrochem. Soc.*, vol. 153, no. 7, pp. A1406–A1416, 2006.
[5] M. Berecibar, I. Gandiaga, I. Villarreal, N. Omar, J. Van Mierlo, and P. Van den Bossche, "Critical review of state of health estimation methods of Li-ion batteries for real applications," *Renew. Sustain. Energy Rev.*, vol. 56, pp. 572–587, Apr. 2016.
[6] M. Chen and G. A. Rincon-Mora, "Accurate electrical battery model capable of predicting runtime and I-V performance," *IEEE Trans. Energy Convers.*, vol. 21, no. 2, pp. 504–511, Jun. 2006.
[7] M. Doyle, T. F. Fuller, and J. Newman, "Modeling of galvanostatic charge and discharge of the lithium/polymer/insertion cell," *J. Electrochem. Soc.*, vol. 140, no. 6, pp. 1526–1533, 1993.
[8] S. J. Moura, "Estimation and control of battery electrochemistry models: A tutorial," in *Proc. IEEE 54th Annu. Conf. Decis. Control (CDC)*, Dec. 2015, pp. 3906–3912.
[9] K. A. Smith, C. D. Rahn, and C.-Y. Wang, "Control oriented 1D electrochemical model of lithium ion battery," *Energy Convers. Manage.*, vol. 48, no. 9, pp. 2565–2578, Sep. 2007.
[10] A. Eddahech, O. Briat, N. Bertrand, J.-Y. Delétage, and J.-M. Vinassa, "Behavior and state-of-health monitoring of Li-ion batteries using impedance spectroscopy and recurrent neural networks," *Int. J. Elect. Power Energy Syst.*, vol. 42, no. 1, pp. 487–494, 2012.
[11] D. Liu, J. Pang, J. Zhou, Y. Peng, and M. Pecht, "Prognostics for state of health estimation of lithium-ion batteries based on combination Gaussian process functional regression," *Microelectron. Rel.*, vol. 53, no. 6, pp. 832–839, 2013.
[12] A. Nuhic, T. Terzimehic, T. Soczka-Guth, M. Buchholz, and K. Dietmayer, "Health diagnosis and remaining useful life prognostics of lithium-ion batteries using data-driven methods," *J. Power Sources*, vol. 239, pp. 680–688, Oct. 2013.
[13] H.-T. Lin, T.-J. Liang, and S.-M. Chen, "Estimation of battery state of health using probabilistic neural network," *IEEE Trans. Ind. Informat.*, vol. 9, no. 2, pp. 679–685, May 2013.
[14] M. Landi and G. Gross, "Measurement techniques for online battery state of health estimation in vehicle-to-grid applications," *IEEE Trans. Instrum. Meas.*, vol. 63, no. 5, pp. 1224–1234, May 2014.
[15] Y. Li, P. Chattopadhyay, A. Ray, and C. D. Rahn, "Identification of the battery state-of-health parameter from input–output pairs of time series data," *J. Power Sources*, vol. 285, pp. 235–246, Jul. 2015.
[16] G.-W. You, S. Park, and D. Oh, "Real-time state-of-health estimation for electric vehicle batteries: A data-driven approach," *Appl. Energy*, vol. 176, pp. 92–103, Aug. 2016.
[17] G.-W. You, S. Park, and D. Oh, "Diagnosis of electric vehicle batteries using recurrent neural networks," *IEEE Trans. Ind. Electron.*, vol. 64, no. 6, pp. 4885–4893, Jun. 2017.
[18] M. T. Hagan, H. B. Demuth, and M. H. Beale, *Neural Network Design*, vol. 20. Boston, MA, USA: Pws Pub., 1996.
[19] S. Ioffe and C. Szegedy, "Batch normalization: Accelerating deep network training by reducing internal covariate shift," 2015, *arXiv:1502.03167*. [Online]. Available: https://arxiv.org/abs/1502.03167

[20] N. Srivastava, G. Hinton, A. Krizhevsky, I. Sutskever, and R. Salakhutdinov, "Dropout: A simple way to prevent neural networks from overfitting," *J. Mach. Learn. Res.*, vol. 15, no. 1, pp. 1929–1958, 2014.
[21] V. Nair and G. E. Hinton, "Rectified linear units improve restricted Boltzmann machines," in *Proc. 27th Int. Conf. Mach. Learn. (ICML)*, 2010, pp. 807–814.
[22] S. Santhanagopalan, Q. Guo, P. Ramadass, and R. E. White, "Review of models for predicting the cycling performance of lithium ion batteries," *J. Power Sources*, vol. 156, no. 2, pp. 620–628, 2006.
[23] G. L. Plett, *Battery Management Systems: Battery Modeling*, vol. 1. Norwood, MA, USA: Artech House, 2015.
[24] P. W. C. Northrop, B. Suthar, V. Ramadesigan, S. Santhanagopalan, R. D. Braatz, and V. R. Subramanian, "Efficient simulation and reformulation of lithium-ion battery models for enabling electric transportation," *J. Electrochem. Soc.*, vol. 161, no. 8, pp. E3149–E3157, 2014.
[25] P. W. C. Northrop, M. Pathak, D. Rife, S. De, S. Santhanagopalan, and V. R. Subramanian, "Efficient simulation and model reformulation of two-dimensional electrochemical thermal behavior of lithium-ion batteries," *J. Electrochem. Soc.*, vol. 162, no. 6, pp. A940–A951, 2015.
[26] M. Torchio, L. Magni, R. B. Gopaluni, R. D. Braatz, and D. M. Raimondo, "LIONSIMBA: A MATLAB framework based on a finite volume model suitable for Li-ion battery design, simulation, and control," *J. Electrochem. Soc.*, vol. 163, no. 7, pp. A1192–A1205, 2016.
[27] EPA. *EPA Urban Dynamometer Driving Schedule (UDDS)*. Accessed: May 2018. [Online]. Available: https://www.epa.gov/emission-standards-reference-guide/epa-urban-dynamometer-driving-schedule-udds

JUNGSOO KIM was born in Seoul, South Korea, in 1988. He received the B.S. degree in mechanical engineering from Korea University, Seoul, in 2013. He is currently pursuing the Ph.D. degree (M.S.-Ph.D. integrated program) with the Department of Creative IT Engineering (CiTE), Pohang University of Science and Technology (POSTECH), Pohang, South Korea. His research interests include Li-ion battery state estimation, Li-ion battery parameter identification, battery management systems (BMSs), and their applications to electric vehicle (EV) and smart grid.

HUIYONG CHUN was born in Seoul, South Korea, in 1994. He received the B.S. degree in electrical engineering from the Pohang University of Science and Technology (POSTECH), Pohang, South Korea, in 2017, where he is currently pursuing the Ph.D. degree in creative IT engineering. His research interests include lithium-ion battery state and parameter estimation, battery management systems, and machine learning applications in lithium-ion battery.

MINHO KIM received the B.S. degree in mechanical engineering from Korea University, Seoul, South Korea, in 2015. He is currently pursuing the Ph.D. degree in creative IT engineering with the Pohang University of Science and Technology (POSTECH), Pohang, South Korea. His main research interests include energy storage systems and machine learning technology.

JUNGWOOK YU received the B.S. degree in information management and technology from Syracuse University, NY, USA, in 2012. He is currently pursuing the Ph.D. degree in creative IT engineering with the Pohang University of Science and Technology (POSTECH), Pohang, South Korea. His research interests include battery management systems, parameter estimation, and neural networks.

KWANGRAE KIM received the B.S. degree in electrical engineering from Konkuk University, Seoul, South Korea, in 2015, and the M.S. degree in electrical engineering from the Pohang University of Science and Technology (POSTECH), Pohang, South Korea, in 2018, where he is currently pursuing the Ph.D. degree in electrical engineering. His research interests include lithium-ion battery state estimation, battery management systems, and optimization applications in battery field.

TAEGYUN KIM received the B.S. and M.S. degrees in electrical engineering from the Pohang University of Science and Technology (POSTECH), Pohang, South Korea, in 2013 and 2016, respectively, where he is currently pursuing the Ph.D. degree in electrical engineering. His main research interest includes the control and management of Li-ion batteries.

SOOHEE HAN received the B.S. degree in electrical engineering and the M.S. and Ph.D. degrees in electrical engineering and computer science from Seoul National University (SNU), Seoul, South Korea, in 1998, 2000, and 2003, respectively. From 2003 to 2007, he was a Researcher with the Engineering Research Center for Advanced Control and Instrumentation, SNU. In 2008, he was a Senior Researcher with the Robot S/W Research Center. From 2009 to 2014, he was with the Department of Electrical Engineering, Konkuk University, Seoul, South Korea. Since 2014, he has been with the Department of Creative IT Engineering, Pohang University of Science and Technology, Pohang, South Korea. His research interests include computer-aided control system designs, distributed control systems, time delay systems, and stochastic signal processing.